Luminescence resulting from electrophoresis of silver particles in water

V. S. Ivanov, B. I. Makshantsev, A. D. Levin, A. V. Bocharov, K. V. Kolchin, I. D. Maleev, and R. A. Perfilov

All-Russian Institute of Optophysical Measurements, 103031 Moscow, Russia
(Submitted 23 May 1995)
Zh. Éksp. Teor. Fiz. **109**, 852–867 (March 1996)

The results are given of an experimental investigation of luminescence detected during electrophoresis between two silver electrodes of silver particles in water that were formed by dissolution of surface layers of the anode. A theoretical interpretation of the experimental data is presented. It is based on the luminescence resulting from recombination of silver ions moving toward the surface of the cathode with electrons tunneling from the cathode from behind the surface. © *1996 American Institute of Physics.* [S1063-7761(96)01103-7]

1. INTRODUCTION

There has recently been a growth of interest in processes involving ions and atoms near the surfaces of solids. Considerable successes have been achieved in developing a theory of such processes.[1–8] Many experimental studies are devoted to the radiation that results from the interaction of ions with the surface of a solid.[9,10] As a rule, the gas phase and high-energy ions are considered. However, there have also been reports of radiation that can be interpreted as radiation resulting from the interaction of slow ions in the liquid phase with the surface of a metal.[11,12]

In this paper, we present the results of an experimental investigation of luminescence observed during the electrophoresis of silver particles dissolved in water. As is demonstrated in the theoretical part of the paper, a possible mechanism of this luminescence is recombination of slow (thermal) ions (the source of which is the silver anode) with electrons that arrive from behind the nominal surface of the silver cathode by below-barrier tunneling. Some of the experiments described below were reported in the preliminary communication of Ref. 11.

2. DESCRIPTION OF THE EXPERIMENTS

In this section of the paper, we describe experiments having as their main aim the direct observation of luminescence that could be interpreted as recombination luminescence resulting from the interaction of slow (thermal) ions with electrons tunneling from a metal near its surface. We attempted to observe luminescence accompanying the electrophoresis of silver particles in an aqueous solution onto the surface of a silver cathode. This method, in particular, makes it possible to solve easily the problem of producing slow (thermal) ions, since silver ions also arise when the silver particles are dissolved in water. The experiment was constructed in such a way as to permit the detection of the luminescence itself and to estimate qualitatively the dynamics of the luminescence in time and also the spectral composition and spatial properties. It was also desirable to have experimentally measured parameters that could be used to estimate the ion concentration. Such a possibility was provided by measurement of the electric current through the solution.

The experimental layout is shown in Fig. 1. Silver electrodes were placed in a quartz-glass flask (1) filled with distilled water obtained by vacuum distillation. In most of the experiments, we used a conical quartz-glass flask (based diameter 70 mm, height 120 mm, thickness of the walls 2.5 mm). Some experiments were also carried out in a cylindrical flask made of ordinary glass. The anode (2) was a ring of diameter 30 mm made from a silver strip of width 2 mm and thickness 0.5 mm, while the cathode (3) took the form of a thin silver disk of diameter 10 mm and thickness 1 mm; both electrodes were placed in the focal plane of the lens (4) (diameter 50 mm, focal length 75 mm).

To detect the expected luminescence, we placed near the flask two FÉU-136 photomultipliers (5 and 6) and a Zenit-E camera (7) with Gelios-40 objective (focal length 85 mm, focal ratio 1:1.5). The camera aperture was left completely open. The distance from the objective lens of the camera to the electrodes was 1000 mm. The camera was focused in such a way as to ensure maximum sharpness of the cathode image.

The beamsplitter (8) was used to divide the light flux from the flask into two parts, one of which was directed onto the photomultiplier (5), which was used for reference purposes, and the second onto the photomultiplier (6), in front of which one of the light filters (9) was placed. To focus the radiation onto the photomultiplier cathodes, the lenses (10 and 11) (diameter 80 mm, focal length 75 mm) were used. All the optical elements listed above were placed in a light-tight box (shown by the dashed line in Fig. 1).

The voltage between the electrodes in the flask was varied between 1 and 30 V from experiment to experiment. In each experiment, the voltage was kept constant. The current in the circuit was monitored by means of the milliammeter (13).

The photomultipliers (5 and 6) operated in the analog regime, and their signals were measured by means of the digital voltmeters (14 and 15). For the photographic detection of the conjectured luminescence, high-sensitivity aerial-photography film (type 29, sensitivity threshold 10^{-7}–10^{-8} J/cm^2) was used.

To estimate the spectral composition of the luminescence, colored glass light filters were used. Compared with prism and diffraction spectral devices, light filters simplify

 1063-7761/96/030458-09$10.00

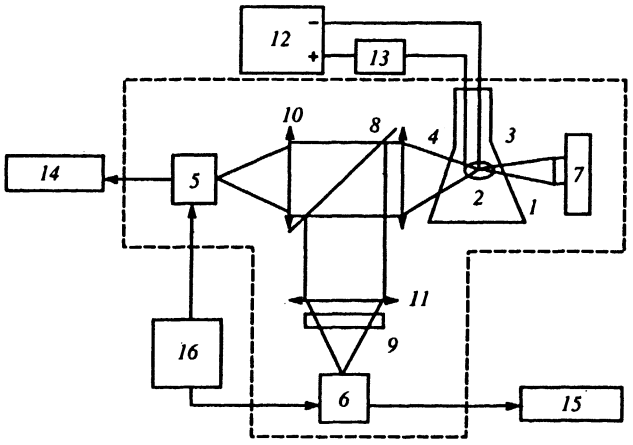

FIG. 1. Experimental layout *1*) quartz flask with distilled water; *2*), *3*) silver electrodes; *4*), *10*), *11*) focusing lenses; *5*), *6*) photomultipliers; *7*) camera; *8*) beamsplitter; *9*) light filter; *12*) power supply ; *13*) milliammeter; *14*), *15*) voltmeters; *16*) power supply for the photomultipliers.

the experiment and ensure a low level of optical losses. The latter is particularly important in the investigation of weak luminescence.

The parameters of the light filters (9), which were stacked in front of the photomultiplier (6), are given in Table I. This set of filters makes it possible to obtain a qualitative idea of the spectral composition of the radiation. Besides the experiments made in accordance with the basic scheme described above, in one of the experiments film was fitted around the outer lateral surface of the flask near the bottom; in the same experiments, film was put beneath the flask.

3. RESULTS OF THE EXPERIMENTS

3.1. Deposition of silver on the inner surface of the flask

A film of metallic silver was deposited on the lateral surface of the conical flask and on its base. The thickness of the film, estimated from the optical absorption, was less than 1 μm.

TABLE I.

Type of filter	Passband, nm (τ_λ>20%)
UFS-8	300–395
BS-4	300–1300
SZS-21	340–580
ZhS-10	400–1800
ZhS-17	480–1800
OS-14	300–2000
KS-19	700–3000

Note: τ_λ is the transmission coefficient of the filter at wavelength λ of the light.

The film was deposited in a horizontal strip in a circle around the flask with randomly varying profile of its upper and lower boundaries. The distance between the boundaries was 10–30 mm. The upper boundary was 1–2 cm above the level of the electrodes. The silver deposited in this film had an almost island structure.

3.2. Deposition of silver on the cathode

During the experiment, the electrophoresis of silver particles onto the cathode was accompanied by the appearance in the region next to the cathode of a formation of suspended disperse particles. In a photograph (see Fig. 2) made in transmitted light after the end of the experiment this formation was readily apparent. It took the form of a jelly with fragile structure and no metallic luster. Within this suspension, individual particles (''droplets'') of metallic silver were observed. The formation of such particles continued for a certain time after the experiment had ceased.

3.3. Luminescence recorded on photographic film

Figure 3 shows photographs indicating the presence of luminescence in the system consisting of the silver electrodes and distilled water. The experiment was carried out using the cylindrical glass flask.

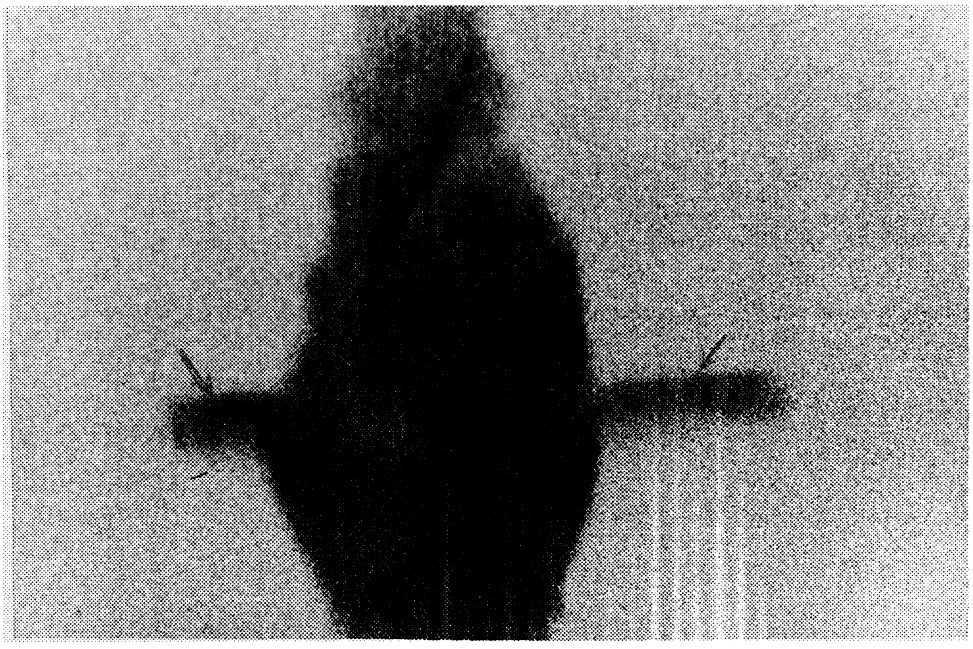

FIG. 2. Side view of the ''jelly'' formed around the cathode and within the anode ring. The anode ring is identified by the arrows.

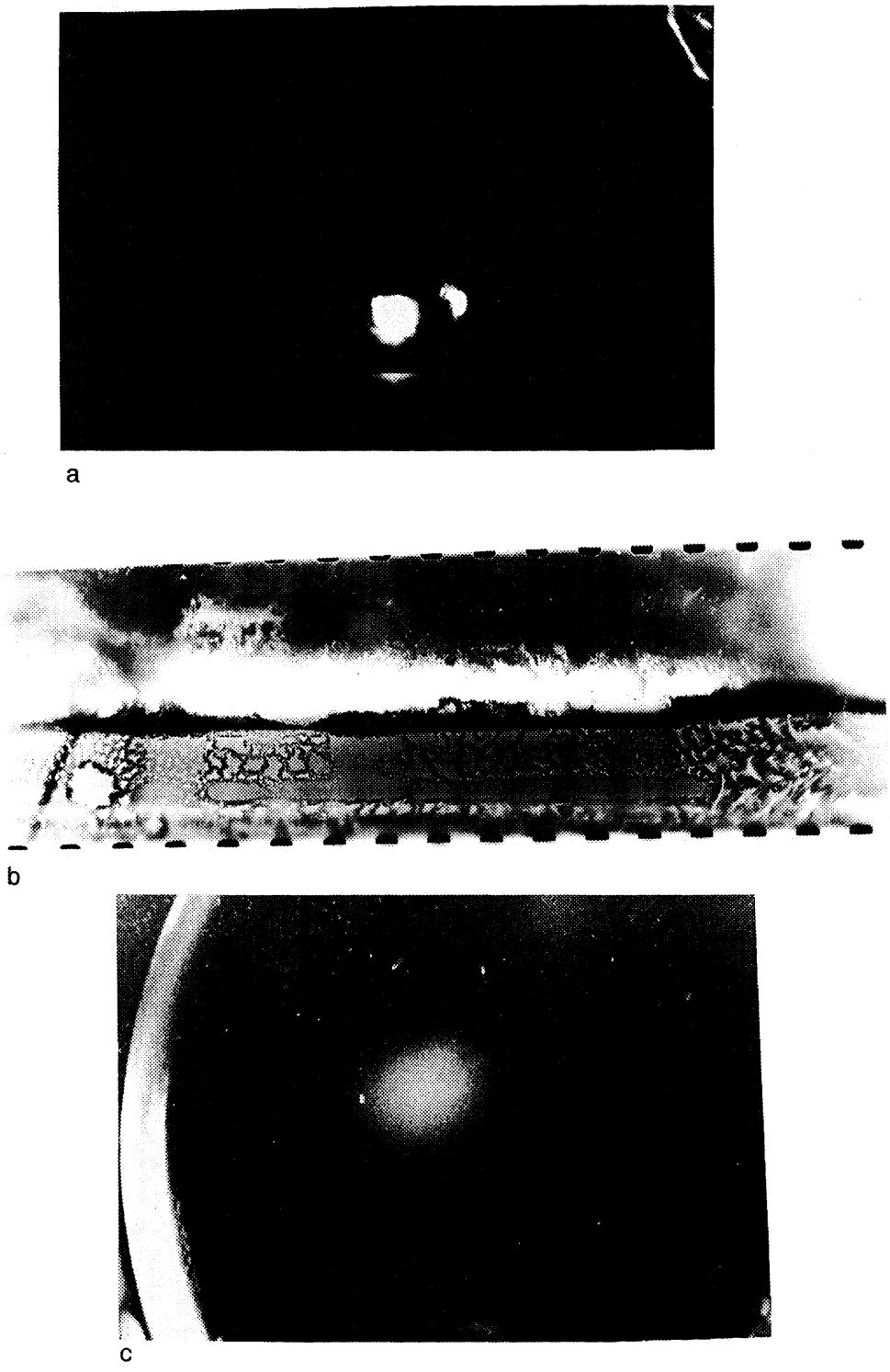

FIG. 3. a) Luminescence around the cathode observed with a camera; b) luminescence observed by means of photographic film wound around the lateral surface of the flask; c) luminescence observed by means of photographic film beneath the flask.

Figure 3a is a photograph obtained by means of the camera focused on the cathode for an exposure of 20 days. During this time, the voltage between the cathodes was held equal to 1 V. Initially the current was about 1 μA. Later it increased, and on the 14th day was 1–5 mA, after which it began to decrease and stopped because the silver anode had dissolved.

In addition, in the same experiment the luminescence was recorded on the films mentioned earlier, one of which was wound round the lateral surface of the flask, while the other was attached to the bottom of the flask (1). The luminescence recorded by these films is shown in Figs. 3b and 3c, respectively. In Fig. 3b, one can clearly see the profiles of silver deposition on the inner surface of the flask.

In another experiment, the voltage between the electrodes was held at 10 V. Figure 4 shows photographs that

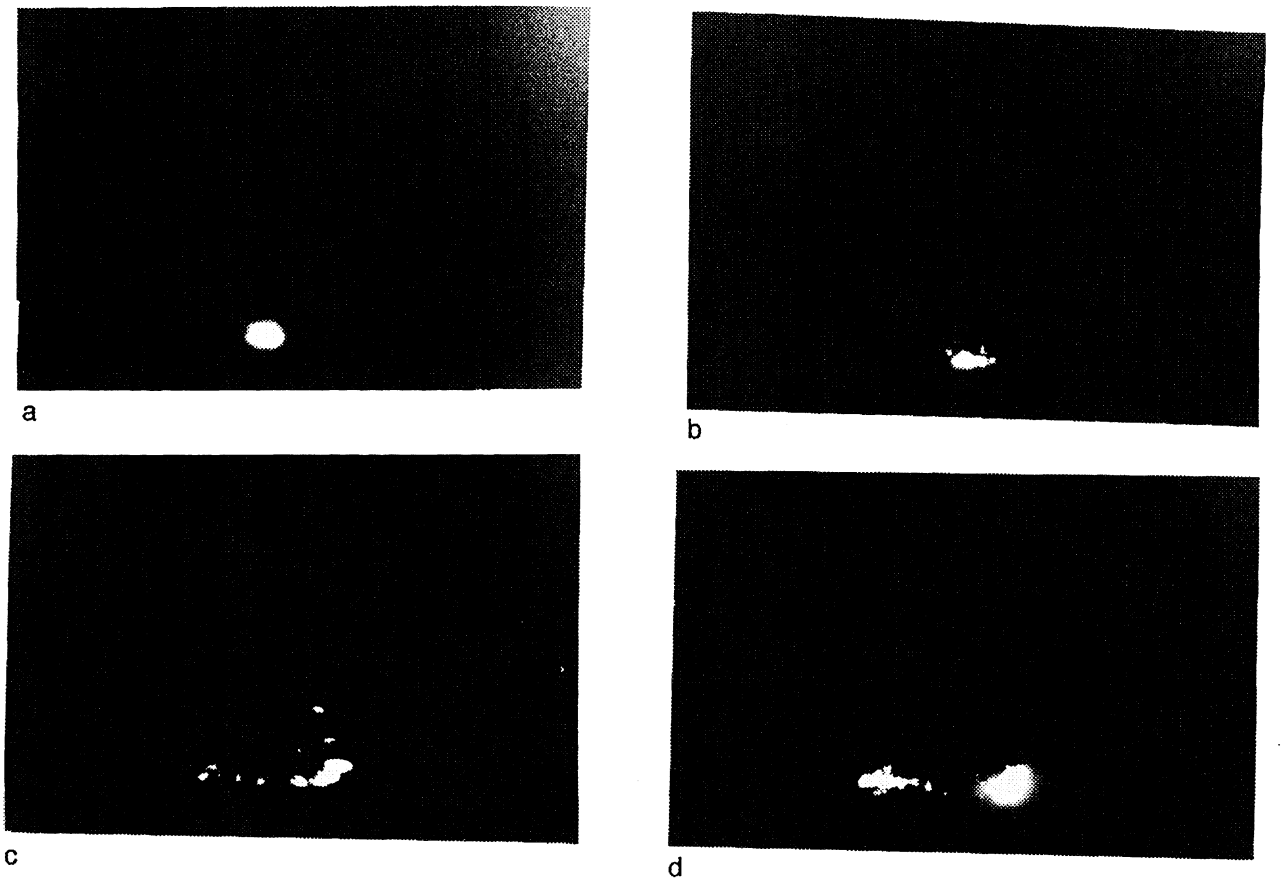

FIG. 4. Luminescence observed by means of the camera during successive time intervals.

demonstrate the presence of luminescence in successive time intervals equal to the exposure time of the corresponding frames. Geometrically, the luminescence is localized in that region of the plane that passes through the anode ring and that cathode. The exposure time of the first frame was 24 h, and that of the remaining frames was 1 h. The time-averaged value of the current was about 5 mA, and it varied from 0.3 mA to 180 mA.

3.4. Luminescence detected by the photomultiplier

3.4.1. Dynamics of the luminescence process

After the experiment began, the photomultiplier did not detect any radiation for a time that was a decreasing function of the voltage between the electrodes. For example, for voltage 10 V between the electrodes, sporadic "bursts" in the readings of the voltmeters (14 and 15 in Fig. 1) up to 0.5–0.7 V began to be observed after a day; these corresponded to an increase in anode current through the photomultipliers to 0.02–0.03 mA. The luminescence was preceded by the onset of a three- to tenfold increase in electric current through the solution. The ending of the photomultiplier signal was accompanied by a sharp decrease in the current to close to the original value. For example, at a certain time the current was 16 mA. For about half an hour it did not change, but then, over 10 s, increased to 180 mA, after which it abruptly fell to 20 mA. At the same time, when the current reached 40 mA, the photomultiplier began to detect luminescence, and this ceased simultaneously with the abrupt decrease in current.

3.4.2. Spectral distribution of the radiation intensity

The spectral distribution of the luminescence was determined from the ratio of the readings of the photomultiplier (6) with different filters to the readings of the reference photomultiplier (5). Allowance was made for the spectral characteristics of the photocathode, the entrance window of the FÉU-136 photomultiplier, and the filters (UFS-8, BS-4, etc., see Table I). The spectral properties of the latter are such that they make it possible to determine the relative intensity of the radiation over comparatively narrow wavelength intervals. This is achieved by subtracting the relative intensities obtained for two suitably chosen filters with subsequent correction of the difference by means of the FÉU-136 spectral characteristic. The experimental results obtained for the spectral distribution of the radiation intensity, normalized to the maximum value, are given in graphical form in Fig. 5. Each point of this graph was obtained by analyzing the data of several measurements. It can be seen that the luminescence has a clear cut short-wavelength edge at $\lambda=350$ nm. Near this wavelength, the spectral density of the radiation has a maximum and then, with increasing wavelength, decreases smoothly.

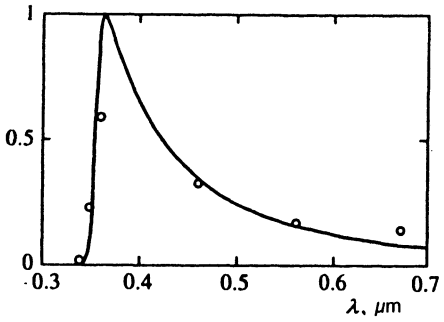

FIG. 5. Experimental spectral distribution of the radiation intensity in the case of deposition of silver ions on the silver cathode (open circles) and the theoretical spectral distribution of the radiation intensity in accordance with the mechanism of recombination luminescence by tunneling electrons (solid curve).

4. DISCUSSION OF THE EXPERIMENTAL RESULTS

The silver deposition processes observed during the experiment are fully consistent with the known physicochemical properties of this metal. All indications are that the silver initially dissolves in the water, forming a colloidal solution (sol). The solution also contains individual silver ions. Under the influence of the electric field, there is then a drift of the colloidal particles, i.e., electrophoresis,[13] and drift of the individual silver ions.

The deposition of silver on the interior lateral surface of the flask and its characteristic features can be explained as follows.

Under the influence of the electric field of the anode ring, the interior surface of the flask acquires a negative charge, the greatest surface density of which will be precisely at the intersection of the plane of the anode ring with the lateral surface of the flask. Because of this, a small fraction of the positively charged silver particles, in particular the individual ions, will move to this region of the inner surface of the flask and be deposited on it. Since the conductivity of the material of the flask is, while admittedly small, nevertheless not equal to zero, some of the charge can be carried off from the interior surface of the flask, so that one can say that this surface has a negative charge.

In addition, a certain number of neutral silver particles, in particular atoms, can be deposited by diffusion in the water to the interior surface of the flask. There will be a higher concentration of these near the anode ring because its surface layer dissolves in the water. It is then natural to expect that neutral particles will be deposited where positively charged silver particles have already begun to be deposited.

The island structure of the deposited silver film can be attributed to the fact that the first layers of silver arise on the surface of the flask material randomly and then subsequently silver particles (including ions and atoms) are preferentially deposited at these locations.

The jelly around the cathode is probably formed by the coagulation of colloidal silver particles. Since the jelly has a certain conductivity, in the later stage of the process, colloidal particles and silver ions are deposited on the surface of this jelly. Such deposition can give rise to the formation of "droplets" of metallic silver, on which, in their turn, positively charged colloidal particles and silver ions moving in the direction from the anode ring to the cathode can be deposited.

The continued formation of "droplets" of metallic silver on the surface of the jelly even after the experiment had ended indicates that the "gel" is indeed formed by silver particles, which under certain conditions can coalesce into "droplets."

The photograph in Fig. 3a reveals luminescence in the vicinity of the cathode; moreover it is in a region situated inside the plane of the cathode ring. This is indicated by the sharp, smooth boundary of the anode ring revealed in the photograph.

The photograph in Fig. 3b also confirms that light is emitted mainly within the anode ring. This is indicated by the presence in the middle of the photograph of a dark strip, which is the silhouette of the anode ring. Below this silhouette is the silver film deposited on the interior surface of the flask. At individual places in this film, one can see the profiles of island formations. These are probably visible because in the early stage of the process the silver film was sufficiently transparent to light emitted inside the flask.

The vertically irregular distribution of the intensity on the film in Fig. 3b can possibley be explained in terms of refraction of radiation from the cathode region by the inhomogeneous distribution of colloidal particles and silver ions in the water.

From the picture of the luminescence recorded by the photograph in Fig. 3c, which is essentially a complementary projection to the picture of the luminescence in Fig. 3b, we can conclude that there are two local sources of luminescence. One is situated within the volume of the flask and emits a rather small amount of light in the direction of its base. The other source is the wall of the flask, and this source yields much more light.

The low intensity of the radiation in the direction of the base of the flask can perhaps also be explained by the fact that the distribution of the densities of the ions and the silver particles in the water is such that refraction of light by this distribution has the consequence that essentially no radiation reaches the bottom.

The radiation from the walls of the flask is evidently mainly radiation that comes from the interior of the flask and is reflected and scattered by the walls. At the same time, a certain fraction of this radiation can propagate to the photographic film through the lateral wall as it does through an optical waveguide. It is also possible that some radiation recorded in the photograph in Fig. 3c is due to the deposition of positively charged silver particles on the interior lateral surface of the flask.

The above considerations enable us to conclude that the luminescence is associated with the deposition of positively charged silver particles on the cathode in the initial stage of the process and then on the surface of the jelly that is formed around the cathode. At the same time, the luminescence sources may well be the droplets of metallic silver on the surface of the jelly.

Evidence for this is provided by the photograph in Fig. 4. We note that the time needed to observe the luminescence

in the experiment recorded in the photographs of Fig. 4 was an order of magnitude less than in the experiment represented by the photographs in Fig. 3. This is due to the fact that the voltage between the electrodes, and therefore the current, was an order of magnitude higher in the first experiment than in the second.

We now discuss the experimental data associated with the luminescence detected by the photomultipliers. The absence of luminescence for one or more days (depending on the voltage between the electrodes) can be explained by an insufficient number of charged silver particles and silver ions in the water. Thus, for voltage 10 V, estimates show that as the silver anode dissolves in the water the concentration of the positively charged silver particles and silver ions reaches some 10^{19} cm^{-3}; the conductivity of the solution is increased, and the current increases to 10 mA. After this, as noted above in Sec. 3.4, the photomultiplier detected sporadic bursts of luminescence accompanied by current pulses. A possible reason for this very nonuniform process of the luminescence in time is that the anode dissolves in the water in discrete chunks as the polar water breaks up its surface. Since the material of the anode is polycrystalline silver, which consists of individual grains (blocks), the separation of individual fragments of the metal occurs most readily along grain boundaries. Thus, an appreciable fraction of the silver dissolved in the water will be in the form of small particles.

When the next chunk of such particles separates from the anode, the particles move toward the cathode and partly dissolve in the water, and this can lead to a sharp increase in the concentration of Ag^+ ions in the water around these particles. This gives rise to an increase in the ionic current. When the same particles, surrounded by a "cloud" of Ag^+ ions, get sufficiently close to the cathode (in the early stage in the process) or to a silver "droplet" on the surface of the "jelly" (at a later stage in the process), the positive charges are neutralized, and the ionic current falls to a value close to the original value.

5. THEORETICAL INTERPRETATION

The above experimental data on the luminescence observed in an experiment involving the deposition in distilled water of positively charge particles of silver and its ions on the surface of a silver cathode can be fully explained by the radiative recombination of electrons tunneling out of the metal with ions moving toward its surface.[11] It should be noted that there are other possible explanations of the observed phenomenon, for example, on the basis of electroluminescence or microscopic electrical breakdown.[14] However, in the present case, such an explanation seems to us less likely, and therefore the theoretical analysis given below takes into account only the mechanics of recombination luminescence of a tunneling electron.

For simplicity, we assume that the ions move in a liquid between two flat electrodes separated by a distance L.

Figure 6 shows schematically the effective potential curves for an electron in a system consisting of the metal and an ion of it near the surface of the metal in a liquid (water) in contact with the metal. We take the effective Hamiltonian of

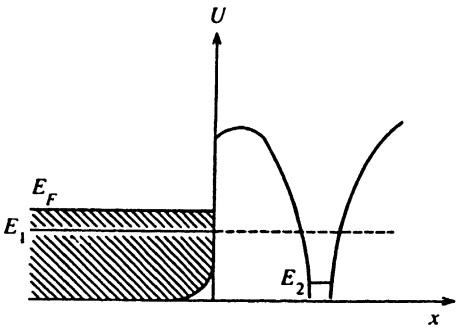

FIG. 6. Schematic potential curves for an electron in a system consisting of a metal and an ion of the same metal.

the electron, with allowance for the presence of the liquid,[15] in a form analogous to that for a metal–vacuum interface:[1]

$$\hat{H}=\hat{H}_1+\hat{H}_2-\hat{T}. \tag{1}$$

Here $\hat{H}_1=\hat{T}-U\theta(-x)$, where $\hat{T}$ is the kinetic energy operator of the electron, U is the effective depth of the potential well of the metal in contact with the liquid, $\theta(-x)=1$ for $x<0$ and $\theta(-x)=0$ for $x>0$,

$$\hat{H}_2=\hat{T}-\frac{Ze^2}{r'}\,\theta(x)$$

is the Hamiltonian of the electron in the effective field of the ion of the metal, which is situated in the liquid at distance x_0 ($x_0>0$) from the nominal boundary $x=0$ of the metal (**e** is a unit vector along the x axis), and

$$|\mathbf{r}'|=r'=|\mathbf{r}-x_0\mathbf{e}_x|.$$

In the effective field of the ion of the metal at distances of the order of atomic distances, Ze can be assumed to be a constant of order e.

The problem is to calculate the spectral distribution of the intensity of the luminescence in accordance with the mechanism of recombination luminescence associated with tunneling of the electron. Such a calculation is possible, since, as will be seen from what follows, the main contribution to this mechanism comes from distances x_0 between the ion and surface of the metal much greater than the atomic distances:

$$x_0\gg a=\hbar^2/mZe^2, \tag{2}$$

where m and e are the effective mass and charge of the electron, and $\hbar$ is Planck's constant. By virtue of (2), the energy levels of the electron states of the ion are well-defined.

We take into account the fact that under the condition (2) and in the absence of liquid between the silver cathode and the silver ion, the levels of the excited electron states of the silver ion are, accordingly to the handbook data of Ref. 16, situated above the Fermi level E_F in silver. Then the completely occupied electron energy levels E_1 in the metal, including the Fermi energy E_F, are greater than the energy E_2 of the electron ground state in the isolated ion. It is natural to assume that this is also true when the liquid is present. One can make estimates that confirm this assumption.

Note that if the excited electron energy levels in the ion are just below the Fermi level in the metal, the expression for the spectral intensity will differ from the expression obtained below only by additional terms that contribute only in the short- and long-wavelength regions of the spectrum.

Taking into account all the above and the circumstance that at ordinary temperatures in the metal almost all the electron states above the Fermi level are free, one can treat the system with the Hamiltonian (1) as a two-level system. The wave functions of the upper, Ψ_i, and lower, Ψ_f, states are determined by the equations

$$\hat{H}\Psi_{i,f}=E_{i,f}\Psi_{i,f}, \tag{3}$$

where $\Psi_{i,f}=a_{i,f}\Psi_i+b_{i,f}\Psi_2$, and E_1 and E_2 are the electron energy in the metal and the ground-state energy of the electron in the field of the ion. In what follows, we measure all energies from the bottom of the potential well of the metal.

Solving Eq. (3) for the region (2), we obtain

$$\Psi_i\approx\Psi_1, \quad E_i\approx E_1, \quad \Psi_f\approx\Psi_2, \quad E_f\approx E_2,$$

where

$$\Psi_i=\begin{cases}\sqrt{2/Sl}\,\sin(k_x l)\exp(-\kappa x+ik_y y+ik_z z), & x\geqslant 0,\\ \sqrt{2/Sl}\,\sin(k_x x+k_x l)\exp(ik_y y+ik_z z), & -l\leqslant x<0,\end{cases} \tag{4}$$

$$\Psi_f=\sqrt{\gamma/\pi}\,\exp(-\gamma r'). \tag{5}$$

Here Sl is the volume of the metal, where S is the area of the electrode;

$$\kappa^2=(2m/\hbar^2)(U-E_i)+k_y^2+k_z^2,$$

$\hbar k_x$, $\hbar k_y$, $\hbar k_z$ are the projections onto the coordinate axes of the electron momentum $\hbar\mathbf{k}$; we can represent $\gamma=1/a=mZe^2/\hbar^2$ in a form that is convenient for what follows:

$$\gamma=\sqrt{2m(U-E_f)}/\hbar.$$

In the calculations below, it is convenient to replace the trigonometric functions in (4) by algebraic functions using the fact that in accordance with (3) we have $\tan(k_x l)=-k_x l$.

To calculate the energy E of the radiation,

$$E=\int_0^\tau dt\int_0^\infty I(\lambda,t)d\lambda, \tag{6}$$

where τ is the emission time, and $I(\lambda,t)$ is the spectral intensity of the recombination radiation as a function of wavelength, we proceed in the usual manner. We first calculate the intensity of the radiation for recombination of electrons with an individual ion. Here we use Fermi's Golden Rule for the transition probability per unit time of the electron from the initial state $|i\rangle$ (4) to the final state $|f\rangle$ (5) under the influence of the electromagnetic field operator:

$$\hat{W}=-\frac{e}{mc}\hat{A}\hat{p}.$$

Here $\hat{A}$ is the vector potential operator of the electromagnetic field, which is taken in the long-wavelength approximation, and $\hat{p}$ is the electron momentum operator.

Multiplying the expression obtained for the intensity of the recombination luminescence associated with the tunneling of electrons by the number $N(x_0,t)Sdx_0$ of ions (or particles around which there is a "cloud" of ions) per volume of liquid Sdx_0 and integrating it over the length L of the intercathode gap, with allowance for the fact that the photon energy is $\hbar\omega=2\pi c\hbar/\lambda$, we obtain for the spectral distribution $I(\lambda,t)$ in (6)

$$I(\lambda,t)=\frac{cS}{2\pi}\int_0^L dx_0 N(x_0,t)\int Vd^3k n_F(E_i(\mathbf{k}))\times\int dE_f\rho(E_f,x_0)\sum_\sigma\int d\Omega V_p\frac{1}{\lambda^5}\times|\langle i,0_{\mathbf{q}\sigma}|\hat{W}|f,1_{\mathbf{q}\sigma}\rangle|^2\delta\left(E_i(\mathbf{k})-E_f-\frac{2\pi c\hbar}{\lambda}\right). \tag{7}$$

Here $V=Sl$; $n_F(E_i(\mathbf{k}))$ is the Fermi distribution function with respect to the initial electron energies in the metal; $\rho(E_f,x_0)$ is the density of the levels of the final electron energies E_f in the ion with allowance for the level smearing due to the interaction of the ion with the liquid and the metal; Ω is the solid angle that determines the direction of the photon polarization vector, which is characterized by the subscript σ, relative to the dipole moment vector of the electron transition between the states $|i\rangle$ (4) and $|f\rangle$ (5); V_p is the volume of the photon subsystem; $0_{\mathbf{q}\sigma}$ and $1_{\mathbf{q}\sigma}$ are the photon occupancies corresponding to the initial ($|i\rangle$) and final ($|f\rangle$) electron states, wave vector $\mathbf{q}$, where $|\mathbf{q}|=2\pi/\lambda$, and polarization σ; $\delta(...)$ is the delta function.

The function $N(x_0,t)$ is determined by the equation

$$\frac{\partial N}{\partial t}=v\frac{\partial N}{\partial x_0}+D\frac{\partial^2 N}{\partial x_0^2}-\beta n(x_0)N \quad (0\leqslant x_0\leqslant L),$$
$$N(x_0=0,t)=0, \quad N(x_0=L,t)=N_0(t). \tag{8}$$

Here v is the velocity of the ion (or of the particle surrounded by a "cloud" of ions), $v=QE/6\pi\eta R$, where Q is the charge of the ion or the ion "cloud," E is the electric field strength, η is the viscosity of the liquid, and R is the radius of the ion (or of the particle surrounded by the ion "cloud"); D is the diffusion coefficient of the ion (or of the particles surrounded by the ion cloud): $D=k_BT/6\pi\eta R$, where k_B is Boltzmann's constant, and T is the temperature. The concentration of the electrons that tunnel from behind the surface of the metal into the liquid is $n(x_0)=n_0\exp(-\gamma' x_0)$, where, as is readily shown,

$$\gamma'=2\sqrt{2m(U-E_F)}/\hbar.$$

As noted above, we are interested in the region $x_0\gg a$. By virtue of this, since $R\sim a$ for the ions, they can be assumed to be point particles, i.e., we can describe their concentration by Eq. (8). It is obvious that if Eq. (8) is also to hold for particles surrounded by an ion "cloud," the inequality $x_0\gg R$ must hold. However, it can be expected that the results will also be qualitatively correct for $x_0>R$.

In Eq. (8), β is the constant that reflects the loss of ions due to nonradiative and radiative recombination with electrons that tunnel out of the metal with ions moving in the liquid toward the metal surface. In the liquid phase, in con-

trast to the gas phase, β is mainly the constant for nonradiative loss of an ion, since an ion of the metal together with the water molecules surrounding it is a complicated entity in which the electron energy is effectively converted nonradiatively into vibrational energy, and subsequently dissipated.

The solution of Eq. (8) can be represented in the form

$$N(x_0,t) = \exp\left(-\frac{vx_0}{2D}\right)\frac{1}{2\pi i}\int_{\varepsilon-i\infty}^{\varepsilon+i\infty} dp e^{pt}\left[A_p K_b\left(\delta\exp\left(-\frac{\gamma' x_0}{2}\right)\right)+B_p I_b\left(\delta\exp\left(-\frac{\gamma' x_0}{2}\right)\right)\right], \quad \varepsilon>0, \tag{9}$$

where

$$A_p = N_0(p)\exp\left(\frac{vL}{2D}\right)\left[K_b\left(\delta\exp\left(-\frac{\gamma' L}{2}\right)\right) - \frac{K_b(\delta)}{I_b(\delta)} I_b\left(\delta\exp\left(-\frac{\gamma' L}{2}\right)\right)\right]^{-1},$$

$$B_p = -\frac{A_p K_b(\delta)}{I_b(\delta)},$$

$$b = \frac{v}{D\gamma'}\sqrt{1+\frac{4Dp}{v^2}}, \quad \delta = \frac{2}{\gamma'}\sqrt{\frac{\beta n_0}{D}}.$$

Here $K_b(...)$ and $I_b(...)$ are cylindrical Bessel functions, and $N_0(p)$ is the Laplace transform of the function $N_0(x_0=L,t)$.

Assuming that $Q\sim 10^{-19}$ C, $E\sim 1$ V/cm, $R\sim a\sim 10^{-8}$ cm, $T\sim 300$ K, $\gamma'\sim 10^8$ cm^{-1}, $\beta\sim 10^{-8}$ cm^3/c, $n_0\sim 10^{22}$ cm^{-3}, and bearing in mind that $L\sim 1$ cm, and for water $\eta\sim 1$ mPa·s, we obtain $v\sim 10^{-3}$ cm/s, $D\sim 10^{-5}$ cm^2/s, and $\delta\sim 100$. It follows from this that $b\ll 1$, $\delta\exp(-\gamma' L/2)\ll 1$, and then for $t\gg 4D/v^2\sim 10$ s, $vx_0/2D\ll 1$, $\delta\exp(-\gamma' x_0/2)\gg 1$, and

$$\pi\delta\exp\left\{-2\delta\left[1-\exp\left(-\frac{\gamma' x_0}{2}\right)\right]-\frac{\gamma' x_0}{2}\right\}\ll 1,$$

and using the asymptotic behavior of the functions $K_b(...)$ and $I_b(...)$ at large and small arguments, we obtain from (9) for the indicated values of x_0

$$N(x_0,t)\approx\sqrt{\frac{2\pi}{\delta}}\frac{v}{\gamma' D}N_0(t)\exp\left[-\delta\exp\left(-\frac{\gamma' x_0}{2}\right)+\frac{\gamma' x_0}{4}\right]. \tag{10}$$

The result (10) does not depend explicitly on the value L of the interelectrode gap. This greatly extends with respect to the parameter R the range of applicability of the calculations made here. Indeed, in the interelectrode gap one will mainly find particles of the metal, including positively charged ones, with radius $R\gg a$. At the same time, as will be shown below, for recombination luminescence in the case of tunneling of electrons the only important charged particles will be those that, approaching the negative cathode or, at later times, the "droplets" of metal on the surface of the jelly, which play the role of a cathode, constitute a complex of an actual metal particle and a "cloud" of ions of the same metal surrounding it. When such a particle is at distance L' from the cathode, where $a\ll L'\ll L$, one can consider the previous problem of recombination luminescence resulting from tunneling in which the role of the charged particles is played by ions with a certain local density $N_0(x=L',t)$ and characteristic radius $R\sim a$. For such a picture of the luminescence, as can be seen from the expressions (7) and (10), the spectrum will not depend on the local concentration of the ions or on the diameters of the metal particles filling the main interelectrode space.

We take into account the fact that the operator $\hat{A}$ has the form

$$\hat{A}=\sum_{\mathbf{q}\sigma}\sqrt{\frac{\hbar c\lambda}{V_p}}\mathbf{e}_\sigma(\mathbf{q})\hat{p}(\hat{a}_{\mathbf{q}\sigma}+\hat{a}^+_{-\mathbf{q}\sigma}),$$

where $\mathbf{e}_\sigma(\mathbf{q})$ is the photon polarization vector, and $\hat{a}_{\mathbf{q}\sigma}$ and $\hat{a}^+_{-\mathbf{q}\sigma}$ are the photon annihilation and creation operators, and also the fact that

$$\langle f|\hat{p}|i\rangle = i\frac{2\pi cm}{\lambda}\langle f|\mathbf{r}'|i\rangle,$$

where $\mathbf{r}'$ is the electron position vector, and also that the density of the energy levels in (7) is $\rho(E_f,x_0)\approx\delta(E_f-E_f^{(0)})$, where $E_f^{(0)}$ is the ground-state energy of the electron in an ion in the liquid far from the surface of the metal. This form of the level density in (7) is due to the fact that the main contribution to the integral over the variable x_0 in (7) comes from values near $x_0\sim(2/\gamma')\ln\delta$, i.e., there is a saddle point, and the main contribution to the luminescence comes from a relatively narrow layer at a distance x_0 that greatly exceeds a.

Taking into account what we have said and also the inequality $\exp[(\gamma-\gamma'/2)x_0]\gg 1$, where $x_0\sim(2/\gamma')\ln\delta$ and $\gamma>\gamma'/2$, since $E_F>E_f=E_f^{(0)}$, we first calculate in (7) the matrix element of the operator $\hat{W}$, then integrate over the variable x, and, finally, integrate over the variables k_x, k_y, k_z. We obtain

$$I(\lambda,t)=\frac{A}{\lambda^2}\sqrt{\left(\Delta-\frac{\lambda_0}{\lambda}\right)\left(\Delta_1+\frac{\lambda_0}{\lambda}\right)}\Gamma\left(\frac{\sqrt{\Delta+\lambda_0/\lambda}}{\ln\delta}\right)\times\frac{\exp(-\sqrt{\Delta-\lambda_0/\lambda})}{1+\kappa'\exp(\lambda_1/\lambda)},$$

$$A=\frac{8\sqrt{\pi}}{3}\frac{e^2\sqrt{(U-E_f^{(0)})^5}SvN_0(t)}{\sqrt{\delta}\sqrt{m^3c^2U\gamma' D}\ln\delta}, \tag{11}$$

$$\Delta=\frac{U-E_f^{(0)}}{U-E_f}\ln^2\delta, \quad \lambda_0=2\pi c\hbar\frac{\ln^2\delta}{U-E_F},$$

$$\Delta_1=E_f^{(0)}\frac{\ln^2\delta}{U-E_F}, \quad \varkappa'=\exp\left(\frac{E_f^{(0)}-E_F}{k_BT}\right), \quad \lambda_1=\frac{2\pi c\hbar}{k_BT},$$

where $\Gamma(...)$ is the incomplete gamma function.

The theoretical spectral intensity (11) of the recombination luminescence in the case of electron tunneling agrees well with the experimental spectral distribution of the luminescence observed in the electrophoresis of silver particles in water onto the silver cathode (Fig. 5). Here the theoretical spectral distribution is normalized to its maximum value and plotted for the following parameter values: $\Delta/\ln^2\delta=1.723$, $\lambda_0/\ln^2\delta=0.257$ μm, $\lambda_1/\ln^2\delta=51.9$ μm, $\Delta_1/\ln^2\delta=0.02$, $\ln\kappa=-145.9$, $\ln\delta=5.118$.

The possibility of invoking recombination luminescence as a result of electron tunneling to explain the experimental data presented in this paper suggests that the emitted energy E (6) must be such that the energy density absorbed by the employed photographic film is not less than its sensitivity threshold: 10^{-7}–10^{-8} J/cm^2. To estimate E from (6) and (11) we have

$$E\sim\frac{A}{\pi c}\frac{\ln\delta}{\delta}\frac{\sqrt{U(U-E_F)}}{\hbar}\int_0^\tau N_0(t)dt. \tag{12}$$

We can estimate $N_0(t)$ from the relation for the current density: $j=eN_0v$. Bearing in mind that $j\sim10^{-3}$–10^{-2} A/cm^2 and $v\sim10^{-3}$ cm/s, we have $N_0\sim10^{19}$–10^{20} cm^{-3}. Further, in accordance with the results of the observation of the luminescence by means of the photomultiplier, the total time of the luminescence "bursts" corresponding to their being recorded in the photographs of Fig. 3 can be estimated to be of the order of 10^4 s. Therefore, for the values of the parameters occurring in the expression (12) that were given above, we obtain for E, setting $U\sim U-E_F\sim10$ eV, the value $E\sim10^{-2}$ J. With allowance for the geometry of the experiment, we obtain for the density of the energy absorbed by the photographic film the value 10^{-6}–10^{-7} J/cm^2, which is sufficient for detection of the luminescence on the film.

It is obvious that the proposed mechanism of the observed luminescence associated with recombination of electrons tunneling out of the metal and ions moving toward its surface explains the observation of luminescence following a sufficient growth of the ionic current, since the probability of recombination luminescence increases with increasing current.

We note that if luminescence via the assumed mechanism is to be efficient, the presence of silver ions, rather than positively charged microscopic particles of the metal, is important. The fact is that if the solution contained only microscopic charged silver particles, then upon approaching the cathode or a "droplet" of metal on the surface of the "jelly," their recombination with electrons tunneling out of the metal would only be nonradiative. This is due to the high concentration of electrons in microscopic metal particles, which carry away the excess energy produced by the recombination of electrons tunneling out of the cathode or a silver "droplet" to a positively charge microscopic particle. This can be understood qualitatively if one bears in mind that in a plasma (in the given case, in the "plasma" of the metal) the radiative recombination rate is proportional to the electron concentration, while the nonradiative recombination rate is proportional to the square of the electron concentration.[17] In contrast, for the recombination of an individual ion with an electron, the probability of nonradiative recombination is many times lower, and accordingly the quantum efficiency of radiative recombination is much higher.

6. CONCLUSIONS

The analysis that we have made in this paper of the experimental data enables us to conclude that luminescence was due to deposition of silver ions on the cathode and that a possible mechanism of the effect could be luminescence resulting from recombination of electrons tunneling out of the cathode with the flux of ions moving toward it. At the least, this is one of the mechanisms that makes it possible to understand the origin of the energy for the luminescence in a system in which all the particles move with velocities corresponding to room temperature and there are no free electrons.

If the luminescence effect found in the condensed medium is due to recombination luminescence of tunneling electrons, it must also occur in the rarefied gas phase. In any event, this is theoretically entirely plausible.

Study of this luminescence can give important information about the structure of the surface electron energy levels in the metal. In addition, study of this effect is also of practical interest. We have in mind here the problem of creating stable and simple reference sources of weak optical radiation and the investigation of the microscopic relief of surfaces.

[1] U. Wille, Phys. Rev. A **45**, 3004 (1992).
[2] A. T. Amos, B. L. Burrows, and S. G. Davison, Surf. Sci. **277**, L100 (1992).
[3] K. Makoshi and H. Kaji, Prog. Theor. Phys. Suppl. **106**, 327 (1992).
[4] H. Kawai, M. Nakayama, and K. Makoshi, Prog. Theor. Phys. Suppl. **106**, 321 (1992).
[5] M. Yu. Gusev, D. V. Klushin, I. F. Urazgil'din, and S. V. Sharov, Zh. Éksp. Teor. Fiz. **103**, 2102 (1993) [JETP **76**, 1047 (1993)].
[6] U. Wille, Surf. Sci. **307–309**, 874 (1994).
[7] J. E. Miraglia, Phys. Rev. A **50**, 2410 (1994).
[8] M. S. Gravielle and J. E. Miraglia, Phys. Rev. A **50**, 2425 (1994).
[9] S. Reinke, D. Rahmann, and R. Hippler, Vacuum **42**, 807 (1991).
[10] C. B. Bargeron, R. A. Murphy, and R. C. Benson, Surf. Sci. **279**, 181 (1992).
[11] B. I. Makshantsev, M. B. Agranat, A. Ya. Aksenov *et al.*, Fiz. Tverd. Tela (Leningrad) **33**, 952 (1991) [Sov. Phys. Solid State **33**, 542 (1991)].
[12] E. P. Koval'chuk, O. M. Yanchuk, and O. V. Reshetnyak, Phys. Lett. A. **189**, 15 (1994).
[13] B. V. Nekrasov, *Handbook of General Chemistry* [in Russian] Khimiya, Moscow (1981).
[14] K. Seeger, *Semiconductor Physics* (Springer-Verlag, Berlin, 1974).
[15] D. Pines and P. Nozieres, Phys. Rev. **109**, 741 (1958).
[16] *Tables of Physical Quantities* [in Russian], I. K. Kikoin (ed.), Atomizdat, Moscow (1976).
[17] Ya. B. Zel'dovich and Yu. P. Raĭzer, *Physics of Shock Waves and High-Temperature Hydrodynamic Phenomena* [in Russian], Fizmatgiz, Moscow (1968), pp. 341–347) [Eng. transl. in two volumes of earlier edition: Academic Press, New York (1966, 1967)].

Translated by Julian B. Barbour